

# EVALUATING AND STEERING MODALITY PREFERENCES IN MULTIMODAL LARGE LANGUAGE MODEL

Yu Zhang<sup>1,2</sup>, Jinlong Ma<sup>1</sup>, Yongshuai Hou<sup>2</sup>, Xuefeng Bai<sup>1</sup>, Kehai Chen<sup>1,2</sup>, Yang Xiang<sup>2</sup>  
Jun Yu<sup>1</sup> & Min Zhang<sup>1,2</sup>

<sup>1</sup>Harbin Institute of Technology, Shenzhen, China

<sup>2</sup>Peng Cheng Laboratory, Shenzhen, China

yuzhang2717@gmail.com, 24s151046@stu.hit.edu.cn

{baixuefeng, chenkehai, yujun, zhangmin2021}@hit.edu.cn

{houysh, xiangy}@pcl.ac.cn

## ABSTRACT

Multimodal large language models (MLLMs) have achieved remarkable success on complex multimodal tasks. However, it remains insufficiently explored whether they exhibit *modality preference*, a tendency to favor one modality over another when processing multimodal contexts. To study this question, we introduce **MC<sup>2</sup>** benchmark, which constructs controlled evidence-conflict scenarios to systematically evaluate modality preference in decision-making. Extensive experiments reveal that all 20 tested MLLMs generally demonstrate clear modality preferences, and such preferences can serve as a useful indicator of downstream task performances of MLLMs. Further analysis shows that modality preference can be controlled by instruction guidance and captured within the latent representations of MLLMs. Built on these insights, we propose a probing and steering method based on representation engineering to explicitly control modality preference without requiring additional fine-tuning. This method effectively amplifies modality preference toward a desired direction and demonstrates promising improvements across multiple downstream applications, including multimodal visual understanding and multimodal machine translation.

## 1 INTRODUCTION

Multimodal Large Language Models (MLLMs; Achiam et al., 2023; Team et al., 2023; Wang et al., 2024; Yin et al., 2024) have emerged as a powerful paradigm for processing and reasoning across heterogeneous data modalities (e.g., text, images, video). Recent advances demonstrate their exceptional capabilities on complex tasks with multimodal contexts, including autonomous web browsing (He et al., 2024), graphical user interface understanding (Hong et al., 2024b), and multimodal dialogue systems (Sun et al., 2022). Despite impressive performance, fundamental questions remain about their *modality preference*—whether MLLMs tend to rely more heavily on one modality than others, and to what extent they favor a specific modality when resolving multimodal inputs.

To investigate this, one line of work (Fu et al., 2024; Amara et al., 2024) compares model performance on unimodal input, providing either only text or only image input for the same question. Another line of research analyzes the relative contributions of textual and visual context, typically by removing one modality to observe the changes of the downstream performance (Park et al., 2025) or Shapley value (Alishahi et al., 2019; Parcalabescu & Frank, 2024; 2022). However, such settings inherently introduce bias, as *they isolate modalities, thus failing to reflect how models process inputs in realistic multimodal scenarios*, where information from different modalities naturally co-occur.

In this paper, we provide a controllable setup to study the modality preference in MLLMs. As shown in the left panel of Figure 1, we introduce a modality context conflict setting, where MLLMs are asked to answer a question based on a pair of contrasting evidence from different modalities. In this

---

The code and data are released at <https://github.com/EchoDreamer/Modality-Preference>.

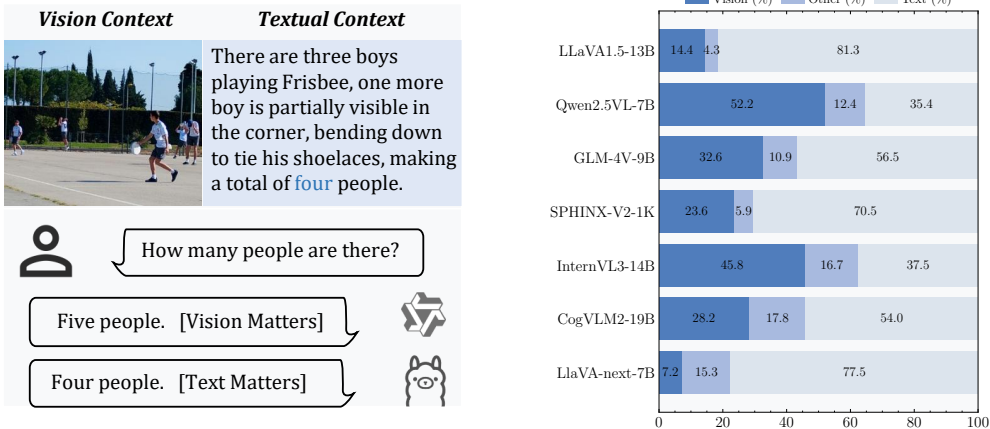


Figure 1: Illustrations of evaluating modality preference. **Left:** Using multimodal conflict context pairs to evaluate modality preference. **Right:** Quantified scores for **Vision** and **Text** modalities, where a higher score indicates a stronger preference toward the corresponding modality. **Other** represents irrelevant predictions, which are discarded during the statistics.

way, we can determine the modality preference based on the answer given by MLLMs. To dismiss the effect of confounding factors including question comprehension, single-modality perception, and the internal knowledge of MLLMs, we annotate and select perception-level tasks that demonstrate accurate question comprehension and reliable single-modality recognition. Building upon this, we introduce a semi-automated annotation framework to construct a refined **Modality Context Conflict** dataset, **MC<sup>2</sup>**, which covers eight perception-level tasks with 2,000 carefully selected samples. Using **MC<sup>2</sup>**, we conduct a comprehensive analysis of modality preference across a diverse set of 20 representative MLLMs. Our study reveals several intriguing findings:

- Most MLLMs (except Qwen2.5-VL and InternVL3) display text preference, as shown in the right panel of Figure 1, and modality preference can serve as a useful indicator of downstream task performances.
- Internal attention patterns toward specific modalities give rise to modality preference, and the underlying factors can be traced to the training data recipe and the scale of the MLLMs.
- Modality preference can be modulated through explicit instruction guidance, and the direction of preference can be captured as geometrically separable patterns in the latent space.

Built on these, we propose a modality preference probing and steering method based on representation engineering (Zou et al., 2023) to explicitly amplify the modality preference without additional fine-tuning. Experimental results show that the proposed method leads to notable performance improvements on multimodal visual understanding and multimodal machine translation. Our main contributions are summarized as follows:

- We introduce **MC<sup>2</sup>** to comprehensively evaluate modality preferences in MLLMs and highlight the significance of modality preference in correlating the downstream task performance.
- Our analysis reveals that intrinsic modality preferences in MLLMs are steerable and identifiable through latent representation, providing insights into multimodal reasoning.
- We propose a training-free method that steers modality preference via representation-level intervention, enabling controllable preference adjustment and enhancing performance on downstream tasks.

## 2 RELATED WORK

### 2.1 MODALITY PREFERENCE

Existing studies on the modality preference of MLLMs can be broadly divided into two categories: 1) investigating the data-related factors that give rise to modality preference or bias, and 2) analyzing the intrinsic characteristics of modality preference within models.

**Data factors influencing modality preference.** Research on data-related factors (Guo et al., 2023; Chen et al., 2024; Leng et al., 2024) explores how properties of multimodal datasets give rise to and reinforce modality preference. In particular, many samples in multimodal datasets can be resolved correctly by relying on information from only a single modality. When prevalent in training data, such samples bias the optimization dynamics, encouraging models to disproportionately rely on a single modality (Chen et al., 2024). Furthermore, their inclusion in evaluation benchmarks artificially inflates performance metrics, as models can exploit these unimodal shortcuts instead of performing genuine cross-modal integration (Leng et al., 2024; Winterbottom et al., 2020). While these studies establish data’s role in inducing preference, our work focuses on exploring the intrinsic modality preference inherent in MLLMs themselves, independent of specific data distributions.

**Evaluating the intrinsic modality preference in MLLMs.** Early studies (Peng et al., 2022; Yang et al., 2024; Wei et al., 2024) analyze modality preference or bias by examining how multimodal models optimize for multimodal inputs. Through such analyses, researchers observe that modality bias has a significant impact on both model optimization and downstream task performance (Peng et al., 2022; Ren et al., 2022; Zhang et al., 2024). While these works offer valuable insights, they typically require training models from scratch, which makes them impractical for large-scale multimodal systems. Recent studies have investigated intrinsic modality preference in MLLMs by evaluating model performance on unimodal inputs—using only text or only image for the same task (Fu et al., 2024; Amara et al., 2024)—and by applying Shapley value-based attribution methods to quantify the contribution of each modality (Alishahi et al., 2019; Parcalabescu & Frank, 2022; 2024). However, in real-world multimodal applications, all modalities are indispensable for task resolution, making these frameworks *inadequate for determining truly modality preference*. Wu et al. (2025) evaluate the model’s ability to detect conflict under scenarios involving conflicting multimodal contexts. However, conflict detection is only one facet of multimodal reasoning and does not comprehensively reflect a model’s modality preference when processing multimodal contexts.

In this work, we simulate multimodal reasoning by examining the behavior of MLLMs in response to questions under scenarios involving conflicting multimodal contexts. Compared to prior work, we carefully control confounding variables such as input quality, question-understanding ability, and internal model knowledge, and construct a modality context conflict dataset, enabling a more rigorous evaluation of modality preference and uncovering new insights. Furthermore, we design a flexible method which can controllably steer the modality preference and demonstrate effectiveness across multiple downstream tasks.

### 2.2 REPRESENTATION ENGINEERING

Extensive research has shown that large language models (LLMs) encode interpretable concepts, such as sentiment, truthfulness, and stylistic attributes in representation space in LLMs (Liu et al., 2023; Panickssery et al., 2023; Subramani et al., 2022; Turner et al., 2023). Building on this foundation, representation engineering has proven effective for editing, enhancing, or suppressing specific behaviors in LLMs (Greenblatt et al., 2023; Stolfo et al., 2024; Wu et al., 2024; Xu et al., 2024; Zou et al., 2023). In this work, we extend this paradigm to a novel setting: controlling modality preference in multimodal large language models (MLLMs). Instead of focusing on abstract properties, our method identifies and manipulates representation directions that are sensitive to modality preference, enabling flexible and targeted control over multimodal reasoning behavior.

## 3 THE MC<sup>2</sup> BENCHMARK

In this section, we introduce the design and methodology behind the construction of the **Multimodal Context Conflict** dataset, **MC<sup>2</sup>**, intended for evaluating modality preference. We outline the data

design philosophy in Section 3.1, followed by the data construction pipeline in Section 3.2 and the question design and evaluation metric in Section 3.3.

### 3.1 DATA DESIGN PHILOSOPHY

To reveal the modality preference of MLLMs when processing truly multimodal inputs, we construct modality context conflict pairs and carefully control various confounding factors that may affect the measurement of modality preference, such as the internal knowledge of MLLMs, question comprehension, and the understanding of unimodal contexts. Therefore, we focus on evaluating perception-level tasks that require minimal external knowledge, reducing the impact of internal knowledge within MLLMs. Besides, we ensure that the evaluated models can accurately answer questions based solely on the context from a single modality, minimizing the influence of confounding factors.

### 3.2 SEMI-AUTOMATED DATA CONSTRUCTION PIPELINE

In this section, we introduce our semi-automated data construction pipeline, which follows a meticulous and iterative process to ensure the robustness and reliability of the dataset, in line with the design philosophy outlined in Section 3.1. The dataset is derived from the TDIUC (Kafle & Kanan, 2017) dataset, sourced from MS-COCO (Lin et al., 2014), widely adopted in model development to ensure the evaluated models can recognize the images. We select the image as vision context  $c^v$ , question  $q$ , and answer  $A^v$  based on the vision context and the image caption  $cap$  for each sample from TDIUC as the foundation for data annotation. The pipeline follows these steps:

**Textual Context Construction.** Given a sample including  $c^v$ ,  $q$ ,  $A^v$  and  $cap$ , we construct candidate contrastive textual contexts  $c^t$  that conflict with  $c^v$  specifically in relation to  $q$  but are aligned with the  $c^v$  and  $cap$  in terms of overall scene semantics. We prompt DeepSeekV3 (Liu et al., 2024a) and ChatGPT4o-mini (Hurst et al., 2024b) to generate a distractor answer  $A^t$  to  $q$ , together with  $c^t$  that plausibly supports  $A^t$ , using carefully crafted instructions.

For each model, we generate two pairs of  $A^t$  and  $c^t$  to facilitate downstream data selection. To ensure that all evaluated MLLMs demonstrate strong recognition capabilities for both visual and textual contexts, we employ several basic MLLMs, such as LLaVA1.5-7B (Liu et al., 2024b) and QwenVL-7B (Bai et al., 2023), as judges to select samples that can be correctly understood with respect to  $c^v$  and  $c^t$ .

**Human Verification.** We incorporate manual inspection to ensure the high quality of the data annotation. Specifically, we verify the existence of conflicts between  $c^v$  and  $c^t$  and ensure that both contexts can correctly direct  $q$  to the corresponding answers,  $A^v$  and  $A^t$ . Each sample is cross-verified by three human annotators to ensure the reliability of the results, and when errors are found, annotators either correct or discard the sample entirely.

**Iterative Refinement.** The dataset undergoes multiple rounds of refinement through a feedback loop between textual context generation and human verification, which helps identify and rectify potential errors, thereby enhancing the dataset quality.

**Modality Context Conflict Dataset.** To this end, we construct **MC<sup>2</sup>**, a modality context conflict dataset including 2000 samples.

The detailed instruction templates for textual context generation, the detailed manual annotation procedures, the data annotation format along with sample cases and dataset statistics are provided in Appendix B.

### 3.3 QUESTION DESIGN AND EVALUATION METRIC

**Question Design.** We reformulate the original questions with ChatGPT-4o-mini (Hurst et al., 2024a) into a binary-choice format. To further reduce potential *position bias* in multimodal inputs, we adopt a *consistent evaluation* strategy, similar to Liu et al. (2024d). Concretely, for each question, we construct two versions by swapping the order of the answer choices. A model’s prediction is regarded as *consistent* only if it selects the same answer in both versions for a sample; otherwise, it is labeled as *inconsistent*. Such inconsistent samples are discarded from the subsequent measurement of modality preference.

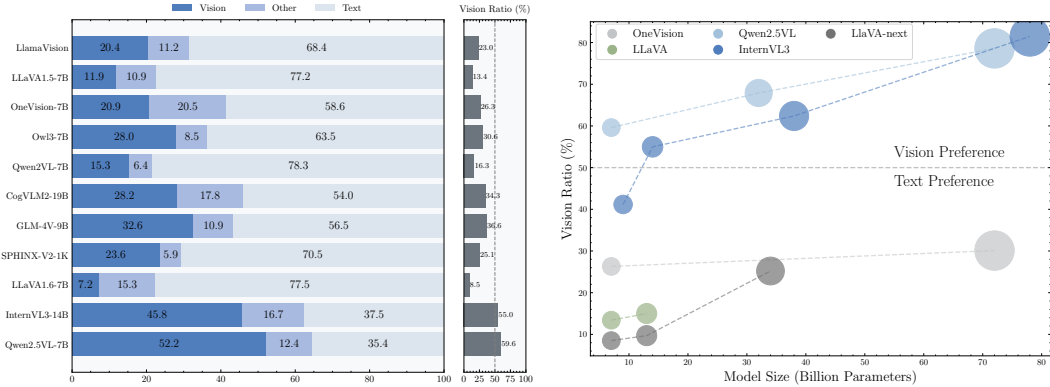


Figure 2: Results of modality preference across different MLLMs. **Left:** Quantified scores for **Vision, Others Text** modalities using  $S_{vision}$ ,  $S_{others}$  and  $S_{text}$  as well as **Vision Ratio**. **Right:** Trends of **Vision Ratio** with respect to model parameter size across different MLLMs.

**Evaluation Metric.** Inspired by prior work on evaluating stylistic or knowledge-related preferences of LLMs and MLLMs through conflict-pair contexts (Li et al., 2024b; Xie et al., 2023; Liu et al., 2025), we extend this idea to evaluate the modality preference by designing a metric that captures how MLLMs respond to conflicting signals from different modalities. More importantly, through the careful design of our benchmark, we establish as a basis that the model can reliably understand both modalities in isolation. As shown in Table 9 and Table 10 in Appendix, all models achieve over 95% accuracy when provided with either textual or visual context.

Building on this, our metric evaluates modality preference by assessing how the model’s responses align with textual or visual input when the two provide conflicting signals. The model’s response is then categorized based on which modality it aligns with: 1) **Vision**: the response aligns with the visual context; 2) **Text**: the response aligns with the textual context; 3) **Others**: the responses are ambiguous, uncertain, or inconsistent with either modality, which are discarded from further analysis. Then, we naturally define the **Vision Ratio** to quantify the model’s preference toward the vision modality, defined as:  $S_{vision}/(S_{vision} + S_{text})$ , where  $S_{vision}$  or  $S_{text}$  denotes the score of the vision or text modality, computed as the proportion of samples whose responses are categorized as **Vision** or **Text** across the dataset.  $S_{others}$  is the proportion of samples whose responses are categorized as **Others**. Vision Ratio greater than 0.5 indicates that the model tends to favor visual context over text.

## 4 MODALITY PREFERENCES IN MLLMS

This section presents a systematic investigation into modality preference in MLLMs, structured around four key research questions: 1) *Which modality do MLLMs prioritize?* 2) *What factors drive these preferences?* 3) *Can the Vision Ratio provide guidance for downstream task performance?* 4) *Can modality preference be controlled?* This investigation helps uncover the underlying mechanisms of modality preference and enables us to apply these insights to downstream tasks.

### 4.1 WHICH MODALITY DO MLLMS PRIORITIZE?

We use the MC<sup>2</sup> benchmark to evaluate the modality preferences of 20 open-source MLLMs and the proprietary ChatGPT-4o-mini (Hurst et al., 2024a), detailed in Appendix C.1.

**Different MLLMs exhibit different modality preferences.** As described in Section 3.3, we quantify modality preference using **Vision Ratio**, with the results presented in the left panel of Figure 2 and detailed in Table 6. We observe that all MLLMs exhibit clear modality preference, with most models showing a strong preference for text; for instance, LLaVA1.5-7B attains only a 13.4% Vision Ratio. This aligns with the previous findings that MLLMs suffer from a severe language prior (Lee et al., 2024; Parcalabescu & Frank, 2024; Wu et al., 2025). Interestingly, the Qwen2.5VL and InternVL3 show a certain degree of preference towards the vision modality.

**Larger MLLMs exhibit stronger preferences for the vision modality.** We evaluate models from the LLaVA1.5, LLaVA-Next, Qwen2.5VL, InternVL3, and LLaVA-OneVision families to investigate the relationship between model size and modality preference. As shown in the right panel of Figure 2, we observe that for all model families, the preference for the vision modality increases with the model size. And the Qwen2.5VL and InternVL3 models exhibit a significant preference for the vision modality once the model size increases. However, LLaVA1.5, LLaVA-Next, and LLaVA-OneVision models maintain a noticeable preference for the text modality as their sizes increase.

**Vision Ratio aligns with human preference.** We further verify whether the Vision Ratio can serve as a human-level measure of modality preference in MLLMs. We randomly sample 100 instances from MC<sup>2</sup> and compute the Vision Ratio of four representative models—Qwen2.5VL-7B, LLaVA-OneVision-7B, InternVL3-14B, and LLaVA1.5-7B. In addition, we craft prompts to elicit explicit reasoning chains from the models, specifically targeting their reliance on visual or textual information. To ensure labeling reliability, three expert annotators independently annotate the expressed modality preference for each response, with the final label determined by majority vote. The automatically obtained Vision Ratio scores ([56.3%, 24.6%, 52.3%, 13.9%]) are highly consistent with the ones given by human ([61.0%, 22.0%, 51.0%, 16.0%]), with an average discrepancy of only 2.68%. This indicates that the Vision Ratio can act as a reliable, automated proxy for human assessment of modality preference.

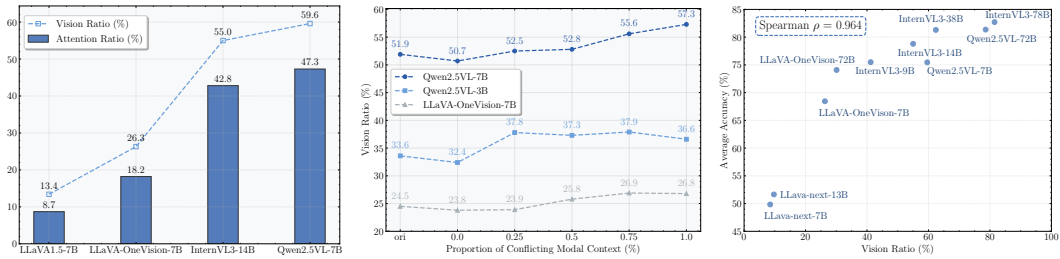


Figure 3: Analysis of modality preferences. **Left:** Trends of Vision Ratio and multimodal Attention Ratio across different models. **Middle:** Vision Ratio with Respect to the Proportion of Multimodal Conflict-Context Training Data and different MLLMs. **Right:** Relationship between visual understanding ability, quantified as the average accuracy across seven widely used benchmarks and the modality preference measured by Vision Ratio.

#### 4.2 WHAT FACTORS DRIVE THESE PREFERENCES?

Given that different MLLMs display varying modality preferences, we examine two primary sources of such differences: *the internal attention distribution* and *the training factors*.

**Different allocation of attention across modalities.** We compute the mean attention scores over all token positions from both modalities and define the ratio of visual attention to total attention as the **Attention Ratio**. By analyzing Qwen2.5VL-7B and LLaVA-OneVision-7B, we observe that the trends of the Attention Ratio closely align with the Vision Ratio across models in the left panel of Figure 3. This alignment suggests that MLLMs distribute attention unevenly between modalities, which in turn contributes to their divergent modality preferences.

**Impact of model scale and training data recipe.** Through reviewing the technical reports of the evaluated MLLMs, we find that they all adopt a common architecture comprising a vision encoder, an alignment layer, and an LLM. Thus, we hypothesize that the observed preferences mainly arise from two factors: 1) Exposure to more multimodal contexts, especially with conflicting cases, drives more pronounced shifts in modality preference. 2) Larger LLMs are more capable of shifting their preference during training;

To examine these hypotheses, we construct a training dataset containing vision–text conflict contexts and fine-tune Qwen2.5VL-7B/3B and LLaVA1.5-7B with varying proportions of samples with multimodal conflict contexts, adjusting their preferences toward text or vision. We then measured changes with the Vision Ratio. We optimize MLLMs in the opposite direction of their original preferences and measure changes using the Vision Ratio. As shown in the middle panel of Figure 3,

increasing the proportion of multimodal contexts consistently leads to larger preference shifts, supporting **Hypothesis 1**. This suggests that multimodal inputs maybe create more challenging training conditions, leading to stronger shifts of preference. Furthermore, Qwen2.5VL-7B exhibites greater shifts than Qwen2.5VL-3B under the same conditions, supporting **Hypothesis 2**. This indicates that larger LLMs demonstrate stronger learning ability and adapt more effectively.

### 4.3 CAN THE VISION RATIO PROVIDE GUIDANCE FOR DOWNSTREAM TASK PERFORMANCE?

To demonstrate the correlation between the modality preference and performance for downstream tasks, we evaluate the visual understanding abilities of 10 representative MLLMs. Specifically, we compute the average accuracy across 7 widely used benchmarks, as detailed in the Appendix C.2. We then compare the visual understanding abilities with their modality preference measured by Vision Ratio using MC<sup>2</sup>, as shown in the right panel of Figure 3. The results reveal a strong positive association between the Vision Ratio and visual understanding ability across the evaluated MLLMs. Specifically, Spearman’s rank correlation (Sedgwick, 2014) reaches  $\rho = 0.964$ , demonstrating that the Vision Ratio provides a highly reliable indicator of visual understanding task performance.

### 4.4 CAN MODALITY PREFERENCE BE CONTROLLED?

We employ instruction guidance to investigate whether modality preference can be controlled, and conduct a latent space representation analysis to examine the mechanisms, underlying the preference adjustment. Details of the experimental design and results are provided in Appendix C.3.

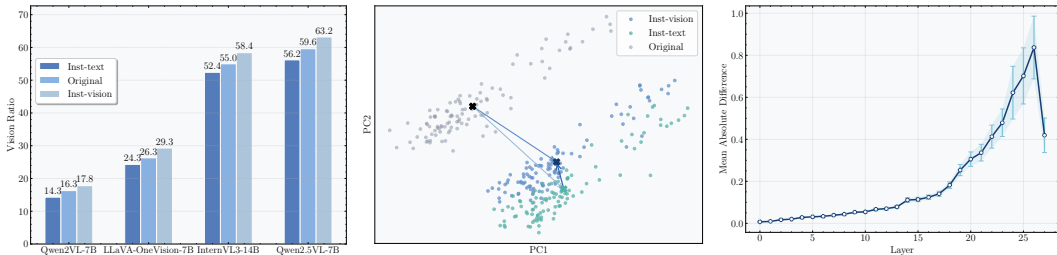


Figure 4: Analysis of modality preference under instruction-guidance. **Left:** Adjustment of modality preference using instruction-guided control (Inst-vision vs. Inst-text). **Middle:** Representation shifts under instruction-guided interventions. **Right:** layer-wise absolute difference and standard deviation of hidden states between different instruction.

**Modality preference can be guided through instruction design.** We investigate the impact of instruction design on modality preference, for instance, by explicitly directing the model to rely on a specific modality when answering a question. Specifically, we evaluate the modality preference measured by Vision Ratio for four representative MLLMs including Qwen2.5VL-7B, LLaVA-OneVision-7B, Qwen2VL-7B and InternVL3-14B under the text or vision preference instruction (Inst-text, Inst-vision). As illustrated in the left panel of Figure 4, instructions that steer the model toward a particular modality effectively shape its modality preference.

**Modality preference direction in representation space.** To further understand how the intervention methods influence modality preference internally, we analyze the hidden representations of the models. Specifically, we apply Principal Component Analysis (PCA; Abdi & Williams, 2010) to the hidden states to identify the dominant direction corresponding to modality preference shifts. The middle panel of Figure 4 shows that instruction-based interventions drive clear shifts in representations, aligning with the modality specified by the instruction. The PCA direction reveals that the model’s internal states are sensitive to modality control cues, which motivates us to develop representation techniques for adjusting modality preference and to apply these insights to downstream tasks in Section 5.

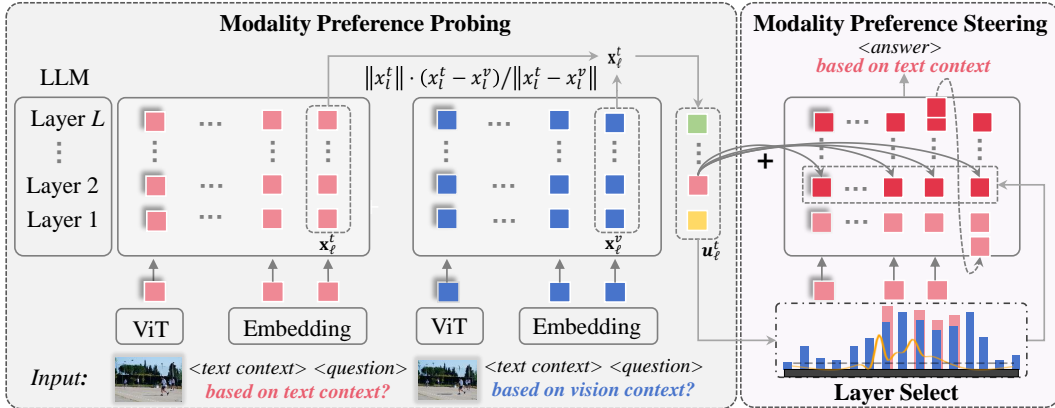


Figure 5: Overall framework of the proposed method. Modality Preference Probing collects the neural activity, computes and scales the direction of modality preference. Modality Preference Steering selects the target layer during the second inference and adds the scaled modality preference direction to the representation at the corresponding layer at each inference step.

## 5 REPRESENTATION BASED MODALITY PREFERENCE STEERING

Inspired by the representation behavior discussed in Section 4.4, we propose to use the representation engineering (Zou et al., 2023) to steer the modality preference, controlling the model’s behavioral expression. As shown in Figure 5, the proposed framework consists of Modality Preference Probing (§5.1) and Modality Preference Steering (§5.2).

### 5.1 MODALITY PREFERENCE PROBING

We probe and collect neural activity that represents the direction of modality preference. Inspired by the pre-training Next Token Prediction objective of decoder-only MLLMs (Hurst et al., 2024a) and the method to extract classification features (Feucht et al., 2024), we collect neural activity from the last token in the input text. The process involves probing modality preference through two pairs of requests: one with a vision preference probing (e.g., ‘answer the question based on the vision context’) and another with a text preference probing (e.g., ‘answer the question based on the text context’). Let us denote these two inputs by  $q^v$  (based on the vision context) and  $q^t$  (based on the text context), and consider a set of  $N$  such pairs  $(q_i^v, q_i^t)$ ,  $i \in \{1, \dots, N\}$ . Let  $\mathbf{x}_{i,\ell}^v, \mathbf{x}_{i,\ell}^t \in \mathbb{R}^d$  be the hidden states on the two queries at the last token of the input at layer  $\ell \in \{1, \dots, L\}$ , where  $d$  is the dimension of the chosen MLLM. We identify the direction of modality preference by computing the difference in the hidden states between the paired inputs. More formally, we compute a vector  $\mathbf{u}_\ell \in \mathbb{R}^d$  representing the direction towards the text modality at layer  $\ell$  for a given query as:

$$\mathbf{u}_\ell^t = \frac{1}{N} \sum_i^N (\mathbf{x}_{i,\ell}^t - \mathbf{x}_{i,\ell}^v). \quad (1)$$

Averaging over different queries allows us to capture the activation values most closely associated with modality preference, independent of questions. As shown in the right panel of Figure 4, we compute the absolute values and standard deviations of the modality preference direction  $\mathbf{u}_\ell^t$  across different samples. We observe that layers 20–23 exhibit both higher absolute values and lower variance, indicating that the preference direction is more prominent and stable in these layers. Based on this observation, we select the corresponding layer  $\ell'$  of the model to control the direction of modality preference in Section 5.2. Similar patterns are observed for Qwen2VL-7B, Qwen2.5VL-7B, LLaVA-OneVision and InternVL3, as detailed in Appendix D.1.

### 5.2 MODALITY PREFERENCE STEERING

After obtaining the probing direction vector, we compute the steering vector by re-scaling the vector  $\mathbf{u}_\ell^t$  with a weight  $w \in \mathbb{R}_d$ . The scaling process must carefully balance two objectives: 1) it must be

Table 1: Performance for steering Qwen2VL-7B and OneVision-7B towards vision modality and steering Qwen2.5VL-7B and InternVL3-8B towards text modality, measured by  $S_{vision}$  and  $S_{text}$ .

Preference	Model	MLLM	InstDesign	CoT	FewShot	Ours
Text↑	Qwen2VL-7B	35.4	37.7	55.6	61.1	63.6
	OneVision-7B	20.9	31.6	36.7	38.2	42.8
Vision↑	Qwen2.5VL-7B	15.3	32.3	34.2	17.2	48.1
	InternVL3-8B	37.5	52.8	53.1	49.8	57.1

Table 2: Multimodal translation results for Ambigcaps (Li et al., 2021). BLEU scores are reported for English (En) ↔ Turkish (Tr).

Method	En->Tr	Tr->En
Qwen2.5VL-7B	8.92	18.56
+Inst towards vision	8.21 (-0.71)	16.09 (-2.47)
+Inst towards text	9.45 (+0.53)	18.98 (+0.42)
+Ours	10.22 (+1.30)	19.89 (+1.33)

Table 3: Performance of the proposed method on the visual understanding benchmark, Phd (Liu et al., 2024c). we report the accuracy results on the phd-icc/phd-iac.

Model	Attribute	Sentiment	Positional	Counting	Object	Avg
Qwen2VL-7B	10.0 / 28.5	2.5 / 8.5	3.5 / 20.5	6.0 / 30.5	8.0 / 50.0	6.0 / 27.6
+InstDesign	14.5 / 34.5	2.5 / 13.0	1.5 / 26.0	5.5 / 39.0	25.0 / 60.0	9.8 / 34.5
+CoT	5.0 / 15.5	6.0 / 23.5	8.5 / 30.2	6.5 / 17.0	40.5 / 59.0	13.3 / 29.0
+FewShot	3.0 / 17.0	0.5 / 9.0	1.5 / 14.5	5.0 / 29.0	2.0 / 37.0	2.4 / 21.3
+Ours	10.0 / 34.4	11.0 / 16.5	14.0 / 28.3	5.0 / 37.4	51.5 / 64.0	<b>18.4 / 36.1</b>
OneVision-7B	11.5 / 20.5	1.5 / 5.0	1.5 / 16.5	6.5 / 28.5	11.0 / 52.0	6.4 / 24.5
+InstDesign	16.0 / 27.0	5.5 / 12.5	6.0 / 31.5	13.5 / 30.5	34.0 / 61.5	15.0 / 32.6
+CoT	17.3 / 28.4	6.2 / 12.9	7.8 / 33.2	13.8 / 30.9	34.5 / 62.1	15.9 / 33.1
+FewShot	17.0 / 28.0	6.0 / 13.0	7.2 / 32.8	13.9 / 31.0	34.8 / 62.3	16.2 / 33.4
+Ours	19.6 / 30.5	7.8 / 13.5	10.3 / 36.4	15.1 / 29.8	35.6 / 63.5	<b>17.7 / 34.7</b>

strong enough to effectively steer the model’s modality preference, 2) it must preserve the model’s normal output behavior. In our preliminary experiments, we observe that setting the weight too large leads to repetitive and meaningless outputs, whereas a too small weight fails to obtain any noticeable change for modality preference. Unlike previous approaches (Zou et al., 2023; Stolfo et al., 2024) that rely on exhaustive search over a validation set to determine the weight, we propose a principled method that aligns the mean of the probed direction distribution with the mean of the original distribution of hidden states. This strategy ensures that the steering remains effective without disrupting the model’s inherent generation capabilities. Formally, the weight is determined by aligning the mean of the probed direction with the central distribution of the original hidden states and the steering vector is computed by:

$$s_{\ell}^t = w \mathbf{u}_{\ell}^t, \text{ where } w = \frac{1}{N} \sum_{i=1}^N \frac{\|\mathbf{x}_{i,\ell}^t\|}{\|\mathbf{u}_{\ell}^t\|} \quad (2)$$

Finally, during the second inference, we adjust the original hidden states at the selected steering layer  $\ell'$  at each decoding step by adding  $s_{\ell'}^t$  to all tokens to steer the model’s response toward the text modality. Similarly, steering models towards vision modality is performed towards the opposite direction. In the final implementation, no additional data or labels are introduced. We only require two consecutive rounds of inference: the first for probing and the second for steering, effectively controlling the modality preference.

### 5.3 EXPERIMENTS

We verify the effectiveness of the method in controlling modality preference on MC<sup>2</sup> and downstream tasks across Qwen2VL-7B, Qwen2.5VL-7B, and LLaVA-OneVision-7B and InternVL3-8B. We consider widely used training-free approaches as baselines: *MLLM* refers to employing MLLM to directly reason in modality-conflicting contexts; *InstDesign* uses instructions to guide modality preference direction; *CoT* enables complex reasoning through intermediate steps; and *FewShot* uses four examples to guide the models. For detailed implementation and results, refer to Appendix D.

As shown in Table 1, the proposed method consistently outperforms the baseline approaches on MC<sup>2</sup> across both settings, demonstrating its effectiveness in adjusting modality preference. We further assess the effectiveness of the proposed method on two types of downstream tasks: 1) multimodal

machine translation (MMT) using AmbigCaps (Li et al., 2021), and 2) visual understanding on PhD (Liu et al., 2024c). The latter includes two subsets—PhD-ica, which contains irrelevant textual context, and PhD-icc, which introduces misleading or incorrect textual information—both of which increase the risk of hallucination. In MMT, the task should primarily ground the source-language text while treating visual information as auxiliary. Accordingly, we adjust modality preference toward the text modality. As shown in Table 2, our method yields an improvement of 1.33 BLEU score over the baselines. By contrast, for PhD, we steer the modality preference toward the vision modality to ground the image. The results in Table 3 demonstrate that our approach achieves substantial improvements across both MLLMs. In particular, when applied to Qwen2VL-7B, our method surpasses the best baseline by an average margin of 6.1 percentage points.

## 6 CONCLUSION

This paper investigates modality preference in multimodal large language models (MLLMs). We carefully curate a modality conflict dataset and use a controlled experimental setup to quantitatively evaluate modality preference. Besides, we find the direction of modality preference can be captured within the latent representations of MLLMs. Inspired by this, we propose a modality preference probing and steering method, which enables significant and flexible changes in modality preference. Experiments show that the proposed method generalizes well to downstream tasks, such as multimodal machine translation and multimodal understanding tasks.

## REFERENCES

- Hervé Abdi and Lynne J Williams. Principal component analysis. *Wiley interdisciplinary reviews: computational statistics*, 2(4):433–459, 2010.
- Josh Achiam, Steven Adler, Sandhini Agarwal, Lama Ahmad, Ilge Akkaya, Florencia Leoni Aleman, Diogo Almeida, Janko Altenschmidt, Sam Altman, Shyamal Anadkat, et al. Gpt-4 technical report. *arXiv preprint arXiv:2303.08774*, 2023.
- Afra Alishahi, Grzegorz Chrupała, and Tal Linzen. Analyzing and interpreting neural networks for nlp: A report on the first blackboxnlp workshop. *Natural Language Engineering*, 25(4):543–557, 2019.
- Kenza Amara, Lukas Klein, Carsten Lüth, Paul Jäger, Hendrik Strobelt, and Mennatallah El-Assady. Why context matters in vqa and reasoning: Semantic interventions for vlm input modalities. *arXiv preprint arXiv:2410.01690*, 2024.
- J Bai, S Bai, S Yang, S Wang, S Tan, P Wang, J Lin, C Zhou, and J Zhou. Qwen-vl: A frontier large vision-language model with versatile abilities. arxiv 2023. *arXiv preprint arXiv:2308.12966*, 2023.
- Shuai Bai, Keqin Chen, Xuejing Liu, Jialin Wang, Wenbin Ge, Sibao Song, Kai Dang, Peng Wang, Shijie Wang, Jun Tang, et al. Qwen2.5-vl technical report. *arXiv preprint arXiv:2502.13923*, 2025.
- Fu Chaoyou, Chen Peixian, Shen Yunhang, Qin Yulei, Zhang Mengdan, Lin Xu, Yang Jinrui, Zheng Xiawu, Li Ke, Sun Xing, et al. Mme: A comprehensive evaluation benchmark for multimodal large language models. *arXiv preprint arXiv:2306.13394*, 3, 2023.
- Meiqi Chen, Yixin Cao, Yan Zhang, and Chaochao Lu. Quantifying and mitigating unimodal biases in multimodal large language models: A causal perspective. *arXiv preprint arXiv:2403.18346*, 2024.
- Zhengxiao Du, Yujie Qian, Xiao Liu, Ming Ding, Jiezhong Qiu, Zhilin Yang, and Jie Tang. Glm: General language model pretraining with autoregressive blank infilling. In *Proceedings of the 60th Annual Meeting of the Association for Computational Linguistics (Volume 1: Long Papers)*, pp. 320–335, 2022.

- Sheridan Feucht, David Atkinson, Byron C Wallace, and David Bau. Token erasure as a footprint of implicit vocabulary items in LLMs. In Yaser Al-Onaizan, Mohit Bansal, and Yun-Nung Chen (eds.), *Proceedings of the 2024 Conference on Empirical Methods in Natural Language Processing*, pp. 9727–9739, Miami, Florida, USA, November 2024.
- Deqing Fu, Ruohao Guo, Ghazal Khalighinejad, Ollie Liu, Bhuwan Dhingra, Dani Yogatama, Robin Jia, and Willie Neiswanger. Isobench: Benchmarking multimodal foundation models on isomorphic representations. *arXiv preprint arXiv:2404.01266*, 2024.
- Aaron Grattafiori, Abhimanyu Dubey, Abhinav Jauhri, Abhinav Pandey, Abhishek Kadian, Ahmad Al-Dahle, Aiesha Letman, Akhil Mathur, Alan Schelten, Alex Vaughan, et al. The llama 3 herd of models. *arXiv preprint arXiv:2407.21783*, 2024.
- Ryan Greenblatt, Buck Shlegeris, Kshitij Sachan, and Fabien Roger. Ai control: Improving safety despite intentional subversion. *arXiv preprint arXiv:2312.06942*, 2023.
- Yangyang Guo, Liqiang Nie, Harry Cheng, Zhiyong Cheng, Mohan Kankanhalli, and Alberto Del Bimbo. On modality bias recognition and reduction. *ACM Transactions on Multimedia Computing, Communications and Applications*, 19(3):1–22, 2023.
- Hongliang He, Wenlin Yao, Kaixin Ma, Wenhao Yu, Yong Dai, Hongming Zhang, Zhenzhong Lan, and Dong Yu. Webvoyager: Building an end-to-end web agent with large multimodal models. *arXiv preprint arXiv:2401.13919*, 2024.
- Wenyi Hong, Weihang Wang, Ming Ding, Wenmeng Yu, Qingsong Lv, Yan Wang, Yean Cheng, Shiyu Huang, Junhui Ji, Zhao Xue, et al. Cogvlm2: Visual language models for image and video understanding. *arXiv preprint arXiv:2408.16500*, 2024a.
- Wenyi Hong, Weihang Wang, Qingsong Lv, Jiazheng Xu, Wenmeng Yu, Junhui Ji, Yan Wang, Zihan Wang, Yuxiao Dong, Ming Ding, et al. Cogagent: A visual language model for gui agents. In *Proceedings of the IEEE/CVF Conference on Computer Vision and Pattern Recognition*, pp. 14281–14290, 2024b.
- Aaron Hurst, Adam Lerer, Adam P Goucher, Adam Perelman, Aditya Ramesh, Aidan Clark, AJ Ostrow, Akila Welihinda, Alan Hayes, Alec Radford, et al. Gpt-4o system card. *arXiv preprint arXiv:2410.21276*, 2024a.
- Aaron Hurst, Adam Lerer, Adam P Goucher, Adam Perelman, Aditya Ramesh, Aidan Clark, AJ Ostrow, Akila Welihinda, Alan Hayes, Alec Radford, et al. Gpt-4o system card. *arXiv preprint arXiv:2410.21276*, 2024b.
- Kushal Kafle and Christopher Kanan. An analysis of visual question answering algorithms. In *Proceedings of the IEEE international conference on computer vision*, pp. 1965–1973, 2017.
- Kang-il Lee, Minbeom Kim, Seunghyun Yoon, Minsung Kim, Dongryeol Lee, Hyukhun Koh, and Kyomin Jung. Vlind-bench: Measuring language priors in large vision-language models. *arXiv preprint arXiv:2406.08702*, 2024.
- Sicong Leng, Yun Xing, Zesen Cheng, Yang Zhou, Hang Zhang, Xin Li, Deli Zhao, Shijian Lu, Chunyan Miao, and Lidong Bing. The curse of multi-modalities: Evaluating hallucinations of large multimodal models across language, visual, and audio. *arXiv preprint arXiv:2410.12787*, 2024.
- Bo Li, Yuanhan Zhang, Dong Guo, Renrui Zhang, Feng Li, Hao Zhang, Kaichen Zhang, Peiyuan Zhang, Yanwei Li, Ziwei Liu, et al. Llava-onevision: Easy visual task transfer. *arXiv preprint arXiv:2408.03326*, 2024a.
- Jiahuan Li, Yiqing Cao, Shujian Huang, and Jiajun Chen. Formality is favored: Unraveling the learning preferences of large language models on data with conflicting knowledge. *arXiv preprint arXiv:2410.04784*, 2024b.

- Jiaoda Li, Duygu Ataman, and Rico Sennrich. Vision matters when it should: Sanity checking multimodal machine translation models. In Marie-Francine Moens, Xuanjing Huang, Lucia Specia, and Scott Wen-tau Yih (eds.), *Proceedings of the 2021 Conference on Empirical Methods in Natural Language Processing*, pp. 8556–8562, Online and Punta Cana, Dominican Republic, November 2021. Association for Computational Linguistics.
- Tsung-Yi Lin, Michael Maire, Serge Belongie, James Hays, Pietro Perona, Deva Ramanan, Piotr Dollár, and C Lawrence Zitnick. Microsoft coco: Common objects in context. In *Computer vision—ECCV 2014: 13th European conference, zurich, Switzerland, September 6–12, 2014, proceedings, part v 13*, pp. 740–755. Springer, 2014.
- Ziyi Lin, Chris Liu, Renrui Zhang, Peng Gao, Longtian Qiu, Han Xiao, Han Qiu, Chen Lin, Wenqi Shao, Keqin Chen, et al. Sphinx: The joint mixing of weights, tasks, and visual embeddings for multi-modal large language models. *arXiv preprint arXiv:2311.07575*, 2023.
- Aixin Liu, Bei Feng, Bing Xue, Bingxuan Wang, Bochao Wu, Chengda Lu, Chenggang Zhao, Chengqi Deng, Chenyu Zhang, Chong Ruan, et al. Deepseek-v3 technical report. *arXiv preprint arXiv:2412.19437*, 2024a.
- Haotian Liu, Chunyuan Li, Yuheng Li, and Yong Jae Lee. Improved baselines with visual instruction tuning. In *Proceedings of the IEEE/CVF Conference on Computer Vision and Pattern Recognition (CVPR)*, pp. 26296–26306, June 2024b.
- Jiazhen Liu, Yuhan Fu, Ruobing Xie, Runquan Xie, Xingwu Sun, Fengzong Lian, Zhanhui Kang, and Xirong Li. Phd: A chatgpt-prompted visual hallucination evaluation dataset. *arXiv preprint arXiv:2403.11116*, 2024c.
- Sheng Liu, Haotian Ye, Lei Xing, and James Zou. In-context vectors: Making in context learning more effective and controllable through latent space steering. *arXiv preprint arXiv:2311.06668*, 2023.
- Xiaoyuan Liu, Wenxuan Wang, Youliang Yuan, Jen-tse Huang, Qiuzhi Liu, Pinjia He, and Zhaopeng Tu. Insight over sight: Exploring the vision-knowledge conflicts in multimodal LLMs. In Wanxiang Che, Joyce Nabende, Ekaterina Shutova, and Mohammad Taher Pilehvar (eds.), *Proceedings of the 63rd Annual Meeting of the Association for Computational Linguistics (Volume 1: Long Papers)*, pp. 17825–17846, Vienna, Austria, July 2025. Association for Computational Linguistics. ISBN 979-8-89176-251-0. doi: 10.18653/v1/2025.acl-long.872. URL <https://aclanthology.org/2025.acl-long.872/>.
- Yuan Liu, Haodong Duan, Yuanhan Zhang, Bo Li, Songyang Zhang, Wangbo Zhao, Yike Yuan, Jiaqi Wang, Conghui He, Ziwei Liu, et al. Mmbench: Is your multi-modal model an all-around player? In *European conference on computer vision*, pp. 216–233. Springer, 2024d.
- Ahmed Masry, Do Xuan Long, Jia Qing Tan, Shafiq Joty, and Enamul Hoque. Chartqa: A benchmark for question answering about charts with visual and logical reasoning. In *ACL Findings*, 2022.
- Nina Panickssery, Nick Gabrieli, Julian Schulz, Meg Tong, Evan Hubinger, and Alexander Matt Turner. Steering llama 2 via contrastive activation addition, 2024. URL <https://arxiv.org/abs/2312.06681>, 2023.
- Letitia Parcalabescu and Anette Frank. Mm-shap: A performance-agnostic metric for measuring multimodal contributions in vision and language models & tasks. *arXiv preprint arXiv:2212.08158*, 2022.
- Letitia Parcalabescu and Anette Frank. Do vision & language decoders use images and text equally? how self-consistent are their explanations? *arXiv preprint arXiv:2404.18624*, 2024.
- Jean Park, Kuk Jin Jang, Basam Alasaly, Sriharsha Mopidevi, Andrew Zolensky, Eric Eaton, Insup Lee, and Kevin Johnson. Assessing modality bias in video question answering benchmarks with multimodal large language models. In *Proceedings of the AAAI Conference on Artificial Intelligence*, volume 39, pp. 19821–19829, 2025.

- Xiaokang Peng, Yake Wei, Andong Deng, Dong Wang, and Di Hu. Balanced multimodal learning via on-the-fly gradient modulation. In *Proceedings of the IEEE/CVF conference on computer vision and pattern recognition*, pp. 8238–8247, 2022.
- Jiawei Ren, Mingyuan Zhang, Cunjun Yu, and Ziwei Liu. Balanced mse for imbalanced visual regression. In *Proceedings of the IEEE/CVF conference on computer vision and pattern recognition*, pp. 7926–7935, 2022.
- Philip Sedgwick. Spearman’s rank correlation coefficient. *Bmj*, 349, 2014.
- Alessandro Stolfo, Vidhisha Balachandran, Safoora Yousefi, Eric Horvitz, and Besmira Nushi. Improving instruction-following in language models through activation steering. *arXiv preprint arXiv:2410.12877*, 2024.
- Nishant Subramani, Nivedita Suresh, and Matthew E Peters. Extracting latent steering vectors from pretrained language models, may 2022. URL <http://arxiv.org/abs/2205.05124>, 2022.
- Qingfeng Sun, Yujing Wang, Can Xu, Kai Zheng, Yaming Yang, Huang Hu, Fei Xu, Jessica Zhang, Xiubo Geng, and Daxin Jiang. Multimodal dialogue response generation. In Smaranda Muresan, Preslav Nakov, and Aline Villavicencio (eds.), *Proceedings of the 60th Annual Meeting of the Association for Computational Linguistics (Volume 1: Long Papers)*, pp. 2854–2866, Dublin, Ireland, May 2022. Association for Computational Linguistics.
- Gemini Team, Rohan Anil, Sebastian Borgeaud, Yonghui Wu, Jean-Baptiste Alayrac, Jiahui Yu, Radu Soricut, Johan Schalkwyk, Andrew M Dai, Anja Hauth, et al. Gemini: a family of highly capable multimodal models. *arXiv preprint arXiv:2312.11805*, 2023.
- Alexander Matt Turner, Lisa Thiergart, Gavin Leech, David Udell, Juan J Vazquez, Ulisse Mini, and Monte MacDiarmid. Activation addition: Steering language models without optimization. *arXiv e-prints*, pp. arXiv–2308, 2023.
- Peng Wang, Shuai Bai, Sinan Tan, Shijie Wang, Zhihao Fan, Jinze Bai, Keqin Chen, Xuejing Liu, Jialin Wang, Wenbin Ge, et al. Qwen2-vl: Enhancing vision-language model’s perception of the world at any resolution. *arXiv preprint arXiv:2409.12191*, 2024.
- Yake Wei, Ruoxuan Feng, Zihe Wang, and Di Hu. Enhancing multimodal cooperation via sample-level modality valuation. In *Proceedings of the IEEE/CVF Conference on Computer Vision and Pattern Recognition*, pp. 27338–27347, 2024.
- Thomas Winterbottom, Sarah Xiao, Alistair McLean, and Noura Al Moubayed. On modality bias in the tvqa dataset. *arXiv preprint arXiv:2012.10210*, 2020.
- Chen Henry Wu, Neil Kale, and Aditi Raghunathan. Why foundation models struggle with cross-modal context. In *ICLR 2025 Workshop on Foundation Models in the Wild*, 2025.
- Muling Wu, Wenhao Liu, Xiaohua Wang, Tianlong Li, Changze Lv, Zixuan Ling, Jianhao Zhu, Cenyuan Zhang, Xiaoqing Zheng, and Xuanjing Huang. Advancing parameter efficiency in finetuning via representation editing. *arXiv preprint arXiv:2402.15179*, 2024.
- X.AI. Grok-1.5 vision preview. <https://x.ai/blog/grok-1.5v>, 2024.
- Jian Xie, Kai Zhang, Jiangjie Chen, Renze Lou, and Yu Su. Adaptive chameleon or stubborn sloth: Revealing the behavior of large language models in knowledge conflicts. In *The Twelfth International Conference on Learning Representations*, 2023.
- Zhihao Xu, Ruixuan Huang, Changyu Chen, and Xiting Wang. Uncovering safety risks of large language models through concept activation vector. *Advances in Neural Information Processing Systems*, 37:116743–116782, 2024.
- Zequn Yang, Yake Wei, Ce Liang, and Di Hu. Quantifying and enhancing multi-modal robustness with modality preference. *arXiv preprint arXiv:2402.06244*, 2024.
- Jiabo Ye, Haiyang Xu, Haowei Liu, Anwen Hu, Ming Yan, Qi Qian, Ji Zhang, Fei Huang, and Jingren Zhou. mplug-owl3: Towards long image-sequence understanding in multi-modal large language models. *arXiv preprint arXiv:2408.04840*, 2024.

- Shukang Yin, Chaoyou Fu, Sirui Zhao, Ke Li, Xing Sun, Tong Xu, and Enhong Chen. A survey on multimodal large language models. *National Science Review*, pp. nwae403, 11 2024. ISSN 2095-5138.
- Xiang Yue, Yuansheng Ni, Kai Zhang, Tianyu Zheng, Ruoqi Liu, Ge Zhang, Samuel Stevens, Dongfu Jiang, Weiming Ren, Yuxuan Sun, et al. Mmmu: A massive multi-discipline multimodal understanding and reasoning benchmark for expert agi. In *Proceedings of the IEEE/CVF Conference on Computer Vision and Pattern Recognition*, pp. 9556–9567, 2024.
- Jinghao Zhang, Guofan Liu, Qiang Liu, Shu Wu, and Liang Wang. Modality-balanced learning for multimedia recommendation. In *Proceedings of the 32nd ACM International Conference on Multimedia*, pp. 7551–7560, 2024.
- Chen Zhe, Wu Jiannan, Wang Wenhai, Su Weijie, Chen Guo, Xing Sen, Zhong Muyan, Zhang Qinglong, Zhu Xizhou, Lu Lewei, Li Bin, Luo Ping, Lu Tong, Qiao Yu, and Dai Jifeng. Internvl: Scaling up vision foundation models and aligning for generic visual-linguistic tasks. In *Proceedings of the IEEE/CVF Conference on Computer Vision and Pattern Recognition*, pp. 24185–24198, 2024.
- Andy Zou, Long Phan, Sarah Chen, James Campbell, Phillip Guo, Richard Ren, Alexander Pan, Xuwang Yin, Mantas Mazeika, Ann-Kathrin Dombrowski, et al. Representation engineering: A top-down approach to ai transparency. *arXiv preprint arXiv:2310.01405*, 2023.

## APPENDICES

All codes, data, and instructions for our MC<sup>2</sup> can be found in <https://anonymous.4open.science/r/Modality-Preference-8016>. MC<sup>2</sup> is released under a Creative Commons Attribution 4.0 License (CC BY 4.0).

Our supplementary materials are summarized as follows:

- Appendix A: Limitations, Social Impacts, Use of LLM and License of Assets.
- Appendix B: Dataset Construction
- Appendix C: Model Evaluation
- Appendix D: Method Applying

## A DISCUSSION

### A.1 LIMITATIONS

This paper investigates the modality preference in multimodal large language models (MLLMs) using a controlled experiment setup with a modality conflict dataset. In constructing the dataset, we employ LLaVA1.5-7B and QwenVL-7B to filter samples and ensure that most models could answer questions correctly based on a single modality. However, this process requires multiple iterations and turned out to be time-consuming. Therefore, devising a more efficient and elegant method for sample selection may be of greater importance.

### A.2 SOCIAL IMPACTS

The proposed MC<sup>2</sup> evaluates the modality preference of MLLMs. Understanding which modality a model prioritizes could be used to circumvent safety mechanisms (e.g., hiding harmful content in the favored modality), making it harder for filters to detect inappropriate content. Therefore, it is essential to incorporate effective safeguards in MLLMs to filter out any inappropriate materials.

### A.3 USE OF LLM

In this work, we use the LLMs including GPT-4o-mini (Hurst et al., 2024a) and DeepSeekV3 (Liu et al., 2024a), and MLLMs including LLaVA1.5-7B (Liu et al., 2024b) and QwenVL-7B (Bai et al., 2023) to help annotate the text context in MC<sup>2</sup>, as detailed in Section B. We evaluate the modality preference of 20 open-source MLLMs and GPT-4o-mini (Hurst et al., 2024a), and steer the modality preference of Qwen2VL-7B (Wang et al., 2024), Qwen2.5VL-7B (Bai et al., 2025), and LLaVA-OneVision-7B (Li et al., 2024a) and InternVL3-8B (Zhe et al., 2024). Besides, we also utilize the LLMs to correct the grammatical errors.

### A.4 LICENSE OF ASSETS

All images in MC<sup>2</sup> are publicly available from COCO (Lin et al., 2014). We release our benchmark under a Creative Commons Attribution 4.0 License (CC BY 4.0) to enhance global accessibility and foster innovation and collaboration in research.

## B DATASET CONSTRUCTION

### B.1 CONFLICT TEXT CONTEXT GENERATION

**Details for data generation using LLMs** To ensure reproducibility and transparency, we include the exact prompts used in our data generation process. These prompts were designed to generate the candidate textual contexts and corresponding answers using GPT-4o-mini (Hurst et al., 2024a) and DeepSeekV3 (Liu et al., 2024a). Below, we provide representative examples of the prompts used during dataset construction given the caption of an image, question, the answer for the question

based on image and the task type for the question. For the full list of prompts, please refer to the project repository.

#### Conflict Context Generation for counting task using DeepSeekV3

Instruction:

# Given a description of an image and a corresponding counting type question with its answer, now you are required to generate a text context that points to an answer that fluctuates by 1 or 2 from the original answer. The context explicitly supports the new answer, providing clear evidence that aligns logically with the counting question. Only one alternative answer should be generated.

Caption: **{caption}**

Question: **{question}**

Answer: **{answer based on vision context}**

Output the new answer enclosed in <answer> </answer> and the context enclosed in <context> </context> tags.

#### Conflict Context Generation of for other tasks using DeepSeekV3

Instruction:

# Given the caption of an image and a corresponding **{task-type}** type question with its answer, now you are required to generate a text context as a premise that supports a new distractor answer for the question. The context should mimic the environment described in the caption but should not include **{answer based on vision context}**, while maintaining logical consistency within the context. Only one alternative answer should be generated.

Caption: **{caption}**

Question: **{question}**

Output the new answer enclosed in <answer> </answer> and the context enclosed in <context> </context> tags.

#### Conflict Context Generation for other tasks using GPT-4o-mini

Instruction:

# Given a caption of an image and a corresponding counting question with its answer, you are required to generate a single text context that provides an indirect premise leading to a new answer that fluctuates by 1 or 2 from the original answer. The context should build an indirect premise to the new answer. Carefully design this context. For this task, I want you to first describe the scene with a certain quantity and then introduce an increase or decrease in that quantity to imply the final answer and don't include the final answer. Only one alternative answer should be generated.

Caption: **{caption}**

Question: **{question}**

Answer: **{answer based on vision context}**

Task-type: **{task-type}**

Output the new answer enclosed in <answer> </answer> and the context enclosed in <context> </context> tags.

## Conflict Context Generation for count task using GPT-4o-mini

Instruction:

# Given the caption of an image and a corresponding question with its answer, now you are required to generate a text context as the indirect premise of a new answer for the question, which belongs to the same category as the original answer. The context should support the new answer, include the caption while maintaining logical consistency within the context and don't include the final answer. Only one alternative answer should be generated.

Caption: {caption}

Question: {question}

Answer: {answer}

Task-type: {task-type}

Output the new answer enclosed in <answer> </answer> and the context enclosed in <context> </context> tags.

**Human Verification** Although the text contexts and answers generated by strong LLMs—filtered through judge MLLMs such as LLaVA1.5-7B (Liu et al., 2024b) and QwenVL-7B (Bai et al., 2023)—generally yield reliable results, we further incorporate manual inspection to ensure the high quality of data annotations. Specifically, we verify that the visual and textual contexts are indeed in conflict, and that each modality independently supports the corresponding answer to the given question. This involves a two-stage manual review process:

- **Modality-Answer Alignment.** First, for each context from different modalities (image and text), annotators assess whether it independently provides sufficient information to correctly answer the question. This step is particularly important because the original VQA answers in the TDIUC (Kafle & Kanan, 2017) dataset may contain error annotations, and the LLM-generated contexts and answers may occasionally be inconsistent.
- **Conflict Verification.** Next, annotators examine whether the visual and textual contexts are semantically inconsistent with respect to the question. That is, the two modalities should lead to different correct answers when considered separately. Samples where both modalities lead to the same answer are discarded, as they do not reflect a true modality conflict.

Samples that do not meet either verification criterion are flagged for further review. Depending on the nature and severity of the issue, we take one of the following actions: revise the prompt to improve clarity, regenerate the problematic part of the sample (e.g., the question or context), or discard the sample entirely if it cannot be reasonably corrected.

To ensure consistency and reduce subjectivity, each category (i.e., vision-aligned, text-aligned, and conflict) is independently verified by three trained annotators. Disagreements are resolved through discussion or majority voting. In addition, we conduct random spot-checks throughout the dataset to ensure the consistency and reliability of the annotations.

Table 4: Average text context length across different task types in the MC<sup>2</sup> dataset.

statistics	Sport	Attribute	Sentiment	Positional	Counting	Color	Activity	Object	Avg
<b>Text Length</b>	52.48	33.50	39.69	31.53	37.12	31.15	49.68	39.71	39.36

## B.2 DATA STATISTICS

We computed the average number of words in the text context for all samples within each task type using the `spacy` library.<sup>0</sup> As shown in Table 4, while there are some variations in text length across tasks, the differences are relatively minor. This indicates that text length is unlikely to be a confounding factor in evaluating modality preference across different task types.

<sup>0</sup>We use the `spacy` library in Python, available at <https://pypi.org/project/spacy/>.

### B.3 ILLUSTRATIVE SAMPLES FROM THE MC<sup>2</sup> BENCHMARK

To provide an intuitive understanding of the MC<sup>2</sup> benchmark and the nature of modality conflict, we present a few representative samples covering different task types as shown in Figure 6, Figure 7, Figure 8 and Figure 9.

<p><b>&lt;image&gt; is a placeholder for below image</b></p>  <p><b>User:</b> &lt;image&gt; <b>Conflict Text Context:</b> <i>Three sheep are peacefully eating grass</i>, surrounded by lush greenery. Their heads are lowered as they nibble on the fresh blades, completely undisturbed. <b>Question:</b> What are the cows in the back doing?  <b>Assistant:</b> &lt;output&gt;  <b>vision-based Answer:</b> <i>running</i>  <b>Text-based Answer:</b> <i>eating</i></p>	<p><b>&lt;image&gt; is a placeholder for below image</b></p>  <p><b>User:</b> &lt;image&gt; <b>Conflict Text Context:</b> In the photo, there are three boys playing Frisbee, and one more boy is partially visible in the corner, bending down to tie his shoelaces, <i>making a total of four people</i>. <b>Question:</b> How many people are in the photo?  <b>Assistant:</b> &lt;output&gt;  <b>vision-based Answer:</b> <i>five</i>  <b>Text-based Answer:</b> <i>four</i></p>
--	--

Figure 6: Illustration of using modality context conflict pairs to investigate modality preference in activity recognition (Left) and counting tasks (Right). The highlighted areas indicate the points of conflict between visual and textual contexts.

## C MODEL EVALUATION

### C.1 EVALUATION DETAIL FOR MODALITY PREFERENCE

We assess open-source multimodal large language models (MLLMs) with different parameter sizes, including LLaVA1.5-7B/13B (Liu et al., 2024b), LLaMA3.2-11B-Vision-Instruct (Grattafiori et al., 2024), LLaVA-OneVision-7B/72B (Li et al., 2024a), CogVLM2-19B (Hong et al., 2024a), mPLUG-Owl3-24-07 (Ye et al., 2024), Qwen2VL-7B (Wang et al., 2024), GLM-4V-9B (Du et al., 2022), SPHINX-V2-1K (Lin et al., 2023), InternVL3-9B/14B/38B/78B (Zhe et al., 2024), LLaVA-next-7B/13B/34B (Liu et al., 2024b) and Qwen2.5VL-7B/32B/72B (Bai et al., 2025). All the open-source models are evaluated using NVIDIA A100 or A800 GPUs. We also evaluate the proprietary model, GPT-4o-mini (Hurst et al., 2024a) via the official API.

**Details of single-modality context evaluation** Before evaluating modality preference, we first assess the ability of MLLMs to answer questions accurately given a single-modality context in the MC<sup>2</sup> dataset. Specifically, we evaluate the models’ accuracy in answering based on text context and based on vision context (based on the image). As shown in Table 9 and Table 10, all models achieve over 95% accuracy when provided with either textual or visual context. This indicates that question understanding and the understanding of single-modality context do not affect the modality preference evaluation. Therefore, we have excluded this confounding factor from the analysis.

**Details of results for modality preference evaluation** We provide the results of modality preference for several models in the left panel of Figure 2 in the main text. More detailed modality preference evaluation results are presented in Table 6.

<image> is a placeholder for below image



**User:** <image> **Conflict Text Context:** *The birthday cake was designed to look like a sleek police car, complete with edible flashing lights and a fondant badge on the side.* **Question:** What is the cake in the shape of?

**Assistant:** <output>  
**vision-based Answer:** *fire truck*  
**Text-based Answer:** *police car*

<image> is a placeholder for below image



**User:** <image> **Conflict Text Context:** *Two wildebeests are standing in a dry, grass-less savanna, their dark coats contrasting with the dusty ground. The area is sparse, with only a few scattered shrubs visible in the background.* **Question:** What animal is shown?

**Assistant:** <output>  
**vision-based Answer:** *zebras*  
**Text-based Answer:** *wildebeests*

Figure 7: Illustration of using modality context conflict pairs to investigate modality preference in attribute recognition (Left) and object recognition tasks (Right). The highlighted areas indicate the points of conflict between visual and textual contexts.

<image> is a placeholder for below image



**User:** <image> **Conflict Text Context:** *A large brown clock tower mounted in the face of a building overlooks a vibrant park filled with lush green trees. The contrast between the brown tower and the surrounding greenery creates a picturesque scene.* **Question:** What color are the trees?

**Assistant:** <output>  
**vision-based Answer:** *white*  
**Text-based Answer:** *green*

<image> is a placeholder for below image



**User:** <image> **Conflict Text Context:** *A white bus with a large rack on the front is parked by the beach, designed to carry equipment for surfing. The rack is sturdy and spacious, perfect for securing bulky items.* **Question:** What can you hang on the rack on the front of the bus?

**Assistant:** <output>  
**vision-based Answer:** *bikes*  
**Text-based Answer:** *surfboards*

Figure 8: Illustration of using modality context conflict pairs to investigate modality preference in color recognition (Left) and positional reasoning (Right) tasks. The highlighted areas indicate the points of conflict between visual and textual contexts.



Figure 9: Illustration of using modality context conflict pairs to investigate modality preference in sentiment understanding and object recognition tasks. The highlighted areas indicate the points of conflict between visual and textual contexts.

### C.2 CAN THE VISION RATIO PROVIDE GUIDANCE FOR DOWNSTREAM TASK PERFORMANCE?

We evaluate the performance of Qwen2.5VL-7B, Qwen2.5VL-72B, InternVL3-9B, InternVL3-14B, InternVL3-38B, InternVL3-78B, LLaVA-OneVision-7B, LLaVA-OneVision-72B, LLaVA-next-7B, LLaVA-next-13B on 7 general multimodal understanding benchmarks including MMMU (Yue et al., 2024), MME (Chaoyou et al., 2023), MMBench (Liu et al., 2024d), RealwordQA (X.AI, 2024), MMStar (Masry et al., 2022), InfoVQA (X.AI, 2024) and ChartQA (Masry et al., 2022). We compute the average score on all datasets, where MME score is normalized between 0-1, as shown in Table 5.

Model	MMMU	MME	MMBench	RealworldQA	MMStar	HallBench	InfoVQA	ChartQA	Avg	Vision Ratio
Qwen2.5VL-7B	58.6	83.8	83.5	68.5	63.9	52.9	82.6	87.3	75.5	59.6
Qwen2.5VL-72B	70.2	87.4	88.6	75.7	70.8	55.2	87.3	89.5	81.4	78.6
InternVL3-9B	57.7	84.7	83.4	70.5	66.3	51.2	79.6	86.2	75.5	41.2
InternVL3-14B	67.1	88.5	85.6	70.7	68.8	55.1	83.6	87.3	78.8	55.0
InternVL3-38B	70.1	90.1	87.6	75.6	71.5	57.1	85.0	89.2	81.3	62.4
InternVL3-78B	72.2	91.1	89.0	78.0	72.5	59.1	86.5	89.7	82.7	81.5
LLaVA-OneVision-7B	47.9	71.2	83.2	66.3	61.7	31.6	68.8	80.0	68.4	26.3
LLaVA-OneVision-72B	55.7	80.8	85.8	71.9	65.8	49.0	74.9	83.7	74.1	30.1
Qwen2VL-7B	54.1	83.1	83.0	70.1	60.7	50.6	76.5	83.0	72.9	16.3
LLaVA-Next-7B	37.6	63.2	69.2	57.8	37.6	27.6	31.6	51.9	49.8	8.5
LLaVA-Next-13B	37.3	62.3	70.0	57.6	40.4	31.8	34.9	59.0	51.6	9.7
LLaVA-1.5-7B	35.7	64.6	69.2	54.8	33.1	27.6	22.4	17.8	42.5	13.4
LLaVA-1.5-13B	37.0	63.6	66.5	55.3	34.3	24.5	24.9	18.5	42.9	15.0

Table 5: Performance comparison across benchmarks for different models measured by accuracy (%) and Vision Ratio score (%).

### C.3 THE DETAILS FOR CONTROLLING MODALITY PREFERENCE

**More results for controlling modality preference through instruction design.** In the left panel of Figure 4, we provide the Vision Ratio results for LLaVA-OneVision-7B, Qwen2.5VL-7B, Qwen2VL-7B and InternVL3-8B. We also present more results on controlling modality preference

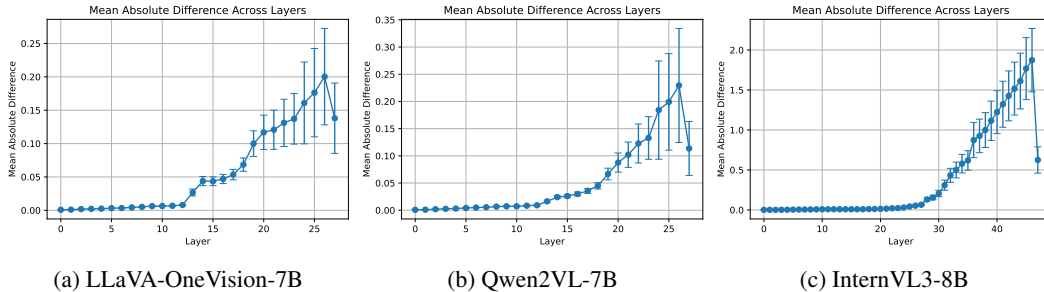


Figure 10: Layer-wise absolute difference and standard deviation of hidden states between image-guided and text-guided instruction for LLaVA-OneVision-7B, Qwen2VL-7B and InternVL3-8B models from left to right.

through instruction design for preference towards the vision modality and the text modality in Table 7 and Table 8. For each setting, we report the results measured by  $S_{vision}$ , vision-based accuracy and  $S_{text}$ , text-based accuracy.

**The details of PCA Analysis** In Section 4.4, we use the PCA analysis regarding the Modality Preference Direction in Representation Space. Here, we provide a more detailed description of the setup. We extract the model’s hidden representations from the last token of the input across different layers. Then, we apply the PCA method to reduce the dimensionality to two dimensions for visualization. The following settings were visualized:

1. The model states under the original modality context input in conflicting scenarios.
2. The model states when there is image noise or textual syntax errors.
3. The model states when specific instructions biased towards image or text are added.

To improve PCA dimensionality reduction efficiency, we selected 500 samples for each setting. Additionally, we calculated the center position after dimensionality reduction for each setting. The center (or centroid) of the samples is computed by taking the mean of the reduced-dimensional points across all the samples.

## D METHOD APPLYING

### D.1 DETAILS FOR PATTERN OF HIDDEN STATES

In the main text, we visualize the layer-wise absolute difference and standard deviation of the hidden states for Qwen2.5VL-7B. As shown in Figure 10, we present the visualization of hidden states for LLaVA-OneVision-7B, Qwen2VL-7B, and InternVL3-8B. For each model, we selected layers with large absolute differences and small standard deviations. This means we identified the layers that showed stable and significant differences between instructions with modality preference towards vision context and text context, which are then used to steer and adjust the model’s modality preference.

### D.2 EVALUATION OF VISUAL UNDERSTANDING AND MULTIMODAL MULTIMODAL MACHINE TRANSLATION

PhD (Liu et al., 2024c) is a visual understanding benchmark and includes two subsets—PhD-ica, which contains irrelevant textual context, and PhD-icc, which introduces misleading or incorrect textual information—both of which increase the risk of hallucination. For testing convenience, we randomly selected 1,000 samples from the original Phd-cc and Phd-ica datasets for evaluation. By steering the model’s modality preference toward the vision modality, we strengthen its visual understanding ability and mitigate vision hallucinations in MLLMs.

Ambigcaps (Li et al., 2021) benchmark explores the role of datasets in stimulating the leverage of the visual modality and proposes methods to highlight the importance of visual signals in the datasets.

Model	Sport	Attribute	Sentiment	Positional	Counting	Color	Activity	Object	Avg
<b>LLaMAVision-11B</b>	31.2/52.4	20.4/69.6	2.0/93.2	21.2/66.8	4.0/93.2	35.2/47.2	10.0/82.4	38.8/42.8	20.4/68.4
<b>LLaVA1.5-7B</b>	20.0/59.6	8.0/88.0	2.0/86.0	8.8/75.2	1.2/96.0	10.8/82.0	9.6/78.8	35.2/52.0	11.9/77.2
<b>LLaVA1.5-13B</b>	34.4/59.6	8.8/89.6	4.8/88.0	12.0/84.8	1.6/96.4	12.8/82.0	9.6/87.6	31.2/62.8	14.4/81.3
<b>OneVision-7B</b>	32.0/36.4	21.6/54.8	2.8/94.4	24.8/56.4	2.4/86.4	30.0/38.0	11.6/71.2	42.4/31.2	20.9/58.6
<b>Owl3-24-07</b>	60.8/31.6	16.4/72.4	10.8/85.6	22.0/69.6	8.4/88.0	28.4/60.4	17.2/71.2	60.0/29.6	28.0/63.5
<b>Qwen2VL-7B</b>	26.4/58.0	12.4/82.8	0.8/95.6	13.2/80.4	4.0/93.6	16.0/78.8	11.6/83.6	38.0/54.0	15.3/78.3
<b>Qwen2.5VL-7B</b>	65.6/12.8	45.2/46.0	18.0/68.8	46.4/38.0	51.6/39.6	70.8/20.0	42.0/43.6	77.6/14.0	52.2/35.4
<b>GLM-4V-9B</b>	42.0/42.4	32.4/59.2	8.8/81.6	28.0/62.4	15.2/74.4	56.8/32.8	23.3/66.0	54.0/32.8	32.6/56.5
<b>SPHINX-V2-1K</b>	39.6/50.8	14.8/82.4	1.2/98.4	16.8/77.6	9.2/85.6	23.2/69.2	24.4/67.2	59.2/32.4	23.6/70.5
<b>InternVL3-9B</b>	45.2/35.2	21.2/68.0	20.8/62.4	27.2/54.4	23.2/50.4	38.0/40.4	19.6/63.2	76.8/14.8	34.0/48.6
<b>InternVL3-14B</b>	72.8/8.8	30.8/48.4	25.2/60.0	33.2/52.0	37.2/47.2	58.0/21.2	24.8/52.8	84.4/9.6	45.8/37.5
<b>CogVLM2-19B</b>	44.0/39.6	29.2/56.0	8.8/75.6	19.2/54.8	8.0/73.2	31.6/43.2	25.2/60.8	59.2/28.4	28.2/54.0
<b>InternVL3-38B</b>	75.2/9.6	45.2/33.6	19.6/60.8	44.0/42.0	41.6/40.0	48.4/29.6	50.4/23.2	84.4/8.0	51.1/30.8
<b>InternVL3-78B</b>	92.4/3.2	46.0/28.8	66.4/18.4	41.6/37.2	69.6/13.2	76.4/8.8	74.4/12.8	89.6/4.0	69.5/15.8
<b>Qwen2.5-VL-32B</b>	85.60/10.40	49.20/39.20	49.60/42.80	52/37.60	52/42	70.80/20	57.20/35.20	86.80/10.40	62.90/29.70
<b>Qwen2.5VL-72B</b>	93.6/4.4	59.2/27.2	50.0/41.2	73.6/19.2	63.6/29.2	83.6/9.6	74.0/21.2	89.2/8.0	73.4/20.0
<b>OneVision-72B</b>	47.2/46.0	20.0/70.8	4.0/93.6	22.8/67.2	12.8/83.2	21.6/60.8	20.8/70.8	71.6/21.2	27.6/64.2
<b>LLaVA1.6-7B</b>	10.8/74.4	5.2/85.2	0.8/93.2	3.6/79.6	0.4/90.8	6.0/76.0	4.8/73.6	26.0/46.8	7.2/77.5
<b>LLaVA1.6-13B</b>	16.0/66.4	7.2/90.4	0.8/92.0	6.4/91.6	2.4/95.6	6.8/88.0	10.0/84.4	22.4/63.2	9.0/84.0
<b>LLaVA1.6-34B</b>	34.8/42.4	12.0/81.6	6.8/85.6	16.8/76.0	11.2/83.2	25.2/60.8	14.0/76.0	60.0/31.6	22.6/67.2
<b>GPT-4o-mini</b>	94.4/3.2	35.6/47.6	60.4/28.4	22.0/58.9	19.4/59.2	34.8/36.4	71.2/20.4	78.4/12.8	52.0/33.4

Table 6: Accuracy of question answering in the MC<sup>2</sup> dataset when both textual and visual contexts are provided but the instruction does not specify which modality context should be used. Values are reported as vision-based accuracy/text-based accuracy for each model.

We evaluate the multimodal machine translation task on this dataset using the Qwen2.5VL-7B model, with different instructions that favor the vision modality and the text modality. Conversely, when guided toward the text modality, the model places greater emphasis on the source language, leading to more accurate grounding in multimodal machine translation. This adjustment prevents the model from over-relying on visual content and from introducing spurious objects or extraneous details into the translation output.

Model	Sport	Attribute	Sentiment	Positional	Counting	Color	Activity	Object	Avg
<b>OneVision-7B</b>	55.6/16.4	31.2/37.2	12.0/76.8	30.8/42.4	3.2/77.6	36.4/18.4	22.4/47.6	61.2/16.4	31.6/41.6
<b>Qwen2VL-7B</b>	60.8/26.8	24.0/69.2	20.0/69.6	20.4/74.0	10.8/80.0	32.0/52.0	27.2/61.6	63.2/28.8	32.3/57.8
<b>Qwen2.5VL-7B</b>	77.6/14.4	43.2/46.8	18.4/72.8	43.2/40.4	35.6/55.6	58.8/24.4	53.6/35.6	81.2/11.6	51.4/37.7
<b>CogVLM2-19B</b>	73.2/13.2	47.6/32.4	35.6/28.4	26.8/45.2	14.0/40.0	61.6/17.6	56.0/28.0	76.0/15.2	48.9/27.5
<b>InternLM-XC2.5-7B</b>	84.0/9.6	46.4/42.8	74.0/18.4	36.0/52.4	22.8/66.0	63.6/20.8	74.0/18.4	76.4/15.6	59.7/30.5
<b>GLM-4V-9B</b>	75.2/18.4	48.8/39.6	28.8/54.0	33.6/55.6	38.4/54.0	76.4/16.4	48.4/38.8	80.0/11.6	53.7/36.1
<b>SPHINX-V2-1K</b>	52.4/38.4	16.4/78.8	2.0/97.2	20.8/72.8	13.6/80.8	30.0/58.8	40.8/52.8	64.8/29.2	30.1/63.6
<b>InternVL3-9B</b>	96.0/2.0	67.2/18.8	82.8/13.2	54.8/26.4	55.6/21.2	84.4/7.6	82.8/6.4	91.6/4.0	76.9/12.4
<b>InternVL3-14B</b>	98.4/0.8	86.0/4.4	87.6/7.6	71.6/12.8	78.0/6.8	97.2/0.8	90.8/3.2	96.4/1.6	88.2/4.8
<b>LLaVA1.6-7B</b>	33.2/54.0	6.8/80.8	6.0/82.4	6.4/79.6	2.8/90.4	10.8/70.0	13.6/69.2	48.4/40.8	16.0/70.9
<b>LLaVA1.6-13B</b>	41.6/40.4	10.4/85.2	4.0/62.8	8.4/83.6	5.6/92.8	14.4/70.8	24.8/58.0	45.2/41.2	19.3/66.9
<b>LLaVA1.6-34B</b>	84.8/12.0	48.0/36.4	62.8/24.0	34.0/52.0	38.8/44.4	76.4/14.4	62.0/18.4	80.4/12.4	60.9/26.8

Table 7: Accuracy of question answering in the MC<sup>2</sup> dataset when both textual and visual contexts are provided and the instruction explicitly directs the model to answer based on visual modality context. Values are reported as vision-based accuracy/text-based accuracy for each model.

Model	Sport	Attribute	Sentiment	Positional	Counting	Color	Activity	Object	Avg
<b>OneVision-7B</b>	45.6/16.4	22.4/37.2	5.6/76.8	27.2/42.4	1.6/77.6	28.8/18.4	16.8/47.6	56.0/16.4	25.5/41.6
<b>Qwen2VL-7B</b>	51.6/34.8	14.8/78.4	6.8/88.0	15.6/79.6	4.0/90.8	18.0/70.8	19.2/72.8	57.6/36.0	23.4/68.9
<b>Qwen2.5VL-7B</b>	77.6/14.4	43.2/46.8	18.4/72.8	43.2/40.4	35.6/55.6	58.8/24.4	53.6/35.6	81.2/11.6	51.4/37.7
<b>CogVLM2-19B</b>	53.6/29.6	28.4/47.6	10.4/56.8	17.6/56.8	6.0/62.0	36.0/35.2	34.0/39.6	67.2/19.6	31.6/43.4
<b>GLM-4V-9B</b>	53.2/32.8	30.4/61.2	6.0/85.6	23.2/68.0	20.0/70.0	52.4/35.6	28.0/60.8	68.0/22.0	35.2/54.5
<b>SPHINX-V2-1K</b>	48.4/41.2	14.4/81.6	2.0/98.0	19.2/77.6	11.2/84.0	27.2/67.2	30.8/65.2	63.2/30.8	27.1/68.2
<b>InternVL3-9B</b>	41.2/27.2	13.6/71.6	22.4/60.8	16.8/64.0	18.0/60.4	25.6/46.4	29.2/49.2	62.4/17.6	28.6/49.6
<b>InternVL3-14B</b>	28.4/44.8	14.0/68.4	3.6/82.4	21.2/54.8	28.0/43.2	24.8/50.0	17.2/58.8	55.2/19.6	24.0/52.8

Table 8: Accuracy of question answering in the MC<sup>2</sup> dataset when both textual and visual contexts are provided and the instruction explicitly directs the model to answer based on the textual modality. Values are reported as vision-based accuracy/text-based accuracy for each model.

Model	Sport	Attribute	Sentiment	Positional	Counting	Color	Activity	Object	Avg
<b>LLaMAVision</b>	97.6	97.2	99.6	99.2	97.2	96.0	97.6	97.6	97.8
<b>LLaVA1.5-7B</b>	98.0	98.0	100.0	97.6	98.4	99.2	97.6	97.6	98.3
<b>LLaVA1.5-13B</b>	97.2	97.6	99.6	97.6	97.6	98.8	95.2	99.2	97.9
<b>OneVision-7B</b>	98.0	95.2	100.0	98.4	98.0	98.8	98.0	100.0	98.3
<b>Owl3</b>	97.6	97.2	99.6	98.8	98.8	99.2	99.2	100.0	98.8
<b>Qwen2VL-7B</b>	98.8	96.4	99.6	99.6	98.8	100.0	98.8	100.0	99.0
<b>Qwen2.5VL-7B</b>	99.2	97.6	100.0	99.6	96.8	98.8	98.4	99.2	98.7
<b>CogVLM2-19B</b>	98.0	95.2	99.2	96.0	94.8	98.4	98.0	99.6	97.4
<b>GLM-4V-9B</b>	98.4	95.2	99.6	97.2	98.8	98.4	99.6	99.6	98.4
<b>SPHINX-V2-1K</b>	98.4	97.6	99.2	98.8	98.0	99.2	98.4	99.6	98.7
<b>InternVL3-9B</b>	97.6	98.0	99.6	99.2	95.6	96.8	98.8	99.2	98.1
<b>InternVL3-14B</b>	98.4	98.4	100.0	99.2	95.6	98.4	98.8	99.6	98.5
<b>InternVL3-38B</b>	97.6	96.8	100.0	98.8	96.0	97.2	98.4	100.0	98.1
<b>InternVL3-78B</b>	97.2	97.6	100.0	98.0	96.4	96.8	98.0	100.0	98.0
<b>Qwen2.5VL-72B</b>	99.6	98.4	96.8	100.0	97.2	100.0	99.6	99.2	98.9
<b>OneVision-72B</b>	100.0	97.6	97.6	99.6	96.4	100.0	100.0	98.8	98.7
<b>GPT-4o-mini</b>	97.6	97.2	99.6	98.6	97.4	98.4	98.4	100.0	98.4

Table 9: Accuracy of question answering in the MC<sup>2</sup> dataset when only unimodal textual context is provided.

Model	Sport	Attribute	Sentiment	Positional	Counting	Color	Activity	Object	Avg
<b>LLaMAVision</b>	100.0	98.8	92.8	98.4	96.4	99.2	98.8	97.2	97.7
<b>LLaVA1.5-7B</b>	99.6	98.0	96.4	100.0	97.6	99.6	98.8	98.4	98.5
<b>LLaVA1.5-13B</b>	99.6	95.2	94.4	97.6	95.2	98.4	96.4	98.4	96.9
<b>OneVision-7B</b>	100.0	97.2	97.2	98.4	84.4	99.6	97.2	98.8	96.6
<b>Owl3</b>	99.2	94.0	94.0	97.2	88.4	96.8	97.2	99.2	95.8
<b>Qwen2VL-7B</b>	99.6	98.8	95.6	98.4	96.4	100.0	99.6	98.4	98.3
<b>Qwen2.5VL-7B</b>	99.6	98.8	98.0	100.0	99.2	100.0	100.0	98.8	99.3
<b>CogVLM2-19B</b>	99.6	99.2	91.2	96.8	91.6	98.8	98.4	98.8	96.8
<b>GLM-4V-9B</b>	99.6	99.2	98.0	99.2	97.6	100.0	99.2	99.6	99.1
<b>SPHINX-V2-1K</b>	98.8	97.6	99.2	92.8	98.0	99.6	96.8	99.2	97.8
<b>InternVL3-9B</b>	98.8	95.6	95.6	96.8	90.0	100.0	98.0	98.0	96.6
<b>InternVL3-14B</b>	99.2	96.4	96.4	98.4	92.4	98.8	97.2	98.4	97.1
<b>InternVL3-38B</b>	100.0	98.0	97.2	100.0	94.4	99.6	99.2	98.8	98.4
<b>InternVL3-78B</b>	99.2	99.6	96.8	98.8	96.0	100.0	99.2	98.4	98.5
<b>Qwen2.5VL-72B</b>	97.2	97.2	100.0	99.2	97.2	98.4	98.4	99.6	98.4
<b>OneVision-72B</b>	100.0	97.6	97.6	99.6	96.4	100.0	100.0	98.8	98.7
<b>GPT-4o-mini</b>	100.0	92.0	95.6	100.0	100.0	96.0	96.4	96.0	97.0

Table 10: Accuracy of question answering in the MC<sup>2</sup> dataset when only unimodal visual context is provided.